Esteves, J.V.; Goushegir, S.M.; dos Santos, J.F.; Canto, L.B.; Hage, E.Jr.; Amancio-Filho, S.T.:

Friction spot joining of aluminum AA6181-T4 and carbon fiber-reinforced poly(phenylene sulfide): Effects of process parameters on the microstructure and mechanical strength

In: Materials and Design (2014) Elsevier

DOI: 10.1016/j.matdes.2014.06.070

Friction spot joining of aluminum AA6181-T4 and carbon fiber-reinforced poly(phenylene sulfide): Effects of process parameters on the microstructure and mechanical strength

J.V. Esteves[1], S.M. Goushegir[2,3], J.F. dos Santos[2] , L.B. Canto[4], E. Hage Jr.[4], S.T. Amancio-Filho[2,3,*]

[1] Graduate Program in Materials Science & Engineering (PPGCEM), Sao Carlos, SP, Brazil.
[2] Helmholtz-Zentrum Geesthacht GmbH, Institute of Materials Research, Materials Mechanics, Solid State Joining Processes, Geesthacht, Germany.
[3] Helmholtz-Zentrum Geesthacht GmbH, Institute of Materials Research, Materials Mechanics, Solid State Joining Processes, Advanced Polymer-Metal Hybrid Structures Group, Geesthacht, Germany.
[4] Federal University of São Carlos (UFSCar), Materials Engineering Department, Sao Carlos, SP, Brazil.

[*] corresponding author: email: sergio.amancio@hzg.de, Tel./Fax: +49 4152 87 2066 /2033

ABSTRACT

Friction spot joining is an alternative technique to produce metal-composite overlap joints. The main process parameters are tool rotational speed, plunge depth, joining time and joining force. In this study, the individual effect of the process parameters on the microstructure and mechanical strength of hybrid AA6181-T4/CF-PPS double lap joints was investigated using Taguchi method and analysis of variance (ANOVA). Produced joints presented mechanical performance from 2107 N to 3523 N. Joints failed by brittle fracture at the interface between aluminum alloy and composite, with displacement-at-peak load values from 0.7 mm to 0.9 mm. Tool rotational speed was the parameter with the largest influence on the joint shear resistance, followed by the joining time, plunge depth and joining force. Higher strength was correlated to the extension of the bonding area and macro-mechanical interlocking related to the formation of a metallic indentation (metallic nub) slightly inserted into the composite. Larger bonding areas were shown to be related to higher heat input (as a result of longer joining times and intermediate rotational speeds) leading to larger consolidate polymeric layers at the metal-composite interface. Higher macro-mechanical interlocking was obtained at larger plunge depths. Joining force was shown to be related to crevice and pore filling of the metal surface by supporting spreading of the molten polymer. Higher joining forces led to better wetting of the interface increasing adhesive forces and joint mechanical performance. Nevertheless excessive joining forces caused squeezing flow of the molten layer reducing joint strength, since a large adhesive area was lost.

Keywords: friction spot joining, hybrid joints, aluminum, composite, design of experiments, Taguchi

1. Introduction

The use of lightweight materials such as aluminum and magnesium alloys and fiber-reinforced plastics has been increased in the transportation industry. This has been supported by the need to decrease weight to meet the strict new environmental regulations to reduce greenhouse gas emissions [1, 2]. As a positive side effect the use of advanced lightweight structures generally decreases fuel consumption, increases vehicle operational range without compromising structural mechanical performance [3, 4]. Because of the technical and economical issues associated with the manufacturing of large structures, the use of dissimilar structural materials has become a common solution in automotive and aircraft applications. This new paradigm in multi-material structures requires the development of advanced joining technologies. Joining of composite-metal structures is a complex task due to the high dissimilarity in material properties, such as thermal resistance and coefficient of thermal expansion [5]. The available techniques to join composite-metal structures are either too expensive, limited in performance or are not environmental friendly [6]. Consequently, there is a niche to be explored in the development of new joining technologies.

Friction spot joining (FSpJ) is an alternative process developed and patented by Helmholtz-Zentrum Geesthacht, Germany [7] for producing metal-polymer overlap spot joints. The process is based on the friction spot welding technology used to weld metals [8,9] and thermoplastics [10,11]. The joining equipment consists of a non-consumable tool with two movable parts - the pin and sleeve - mounted coaxially to a clamping ring, whose function is to ensure contact between the joint partners and avoid material losses [10]. Figure 1a shows the FSpJ tool parts used in this work.

The process can be divided into three steps [7, 12]. In step 1 (Fig. 1b-1) the joining parts are overlapped - metal onto the polymer composite - and fixed by the clamping ring against a hydraulic piston working as a backing bar. Pin and sleeve start to rotate in the same direction with a preset rotational speed. Sleeve slightly plunges into the metallic plate with a preset depth while pin is retracted. The heat generated by the friction between the sleeve and metallic plate plasticizes a volume of metal around the tool. Sleeve feeding induces flow of the plasticized metal, which is driven upwards to the annular space (reservoir) created by the retraction of the pin. In step 2 (Fig.1b-2), the pin and sleeve return back to the surface of metallic plate while the pin pushes down the plasticized metal, refilling the spot area. The tool plunging movement deforms the heated and partially plasticized metallic part at the interface, creating an undercut geometry resembling a metallic "nub". The metallic nub is slightly inserted into the composite plate as can be seen schematically in Figure 1b-3. In step 3 (Fig.1b-3) clamping pressure is released, the tool is removed from the metal plate surface, and the joint consolidates under cooling.

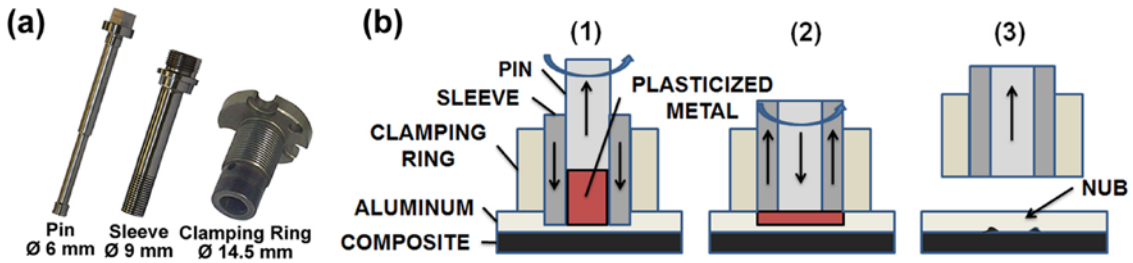

Figure 1: (a) FSpJ tool pieces used in this work. (b) Representation of the FSpJ process steps: 1 - Sleeve plunging into the metallic plate; 2 - Spot refilling; 3 - Joint consolidation under cooling.

The two main bonding mechanisms in friction spot joint of metal-thermoplastic fiber-reinforced composite are [12, 13]: 1) macro-mechanical interlocking due to the nub formation and 2) adhesion forces owing to the micro-scale filling of metal surface crevices and pores by molten polymer and partial exposed fiber entrapment by the plasticized metal at the interface. During the joining process, generated frictional heat is transferred from metal to the composite by conduction, thereby melting a thin layer of the polymeric matrix. The molten layer induces adhesion forces between joining parts after consolidation. Concomitantly fiber bundles in the composite surface may be exposed to the plasticized metal; micro-mechanical anchoring of the fiber by the metal may locally take place, contributing to increase micro-mechanical interlocking [13].

The four main controllable process parameters of the FSpJ technique are: tool rotational speed (RS), joining time (JT), sleeve plunge depth (PD) and joining force (JF). These process parameters directly influence the bonding mechanisms and consequently the microstructure and mechanical performance of the joints. Briefly, rotational speed and joining time control the heat input and the amount of generated polymer molten layer as well as its viscosity. Plunge depth is responsible for the shape and depth of the metallic nub, while joining force ensures intimate contact between the plates and controls the flow of the polymer molten layer.

Previous works have shown the technical feasibility of FSpJ process on hybrid metal-composite joints of lightweight alloys such as magnesium AZ31 [12], aluminum AA2024 [13] and AA6181 [14] with glass and carbon fiber-reinforced thermoplastic composites. These joints showed similar or superior mechanical strength compared to other metal-polymer hybrid joints produced with state-of-the-art techniques. Goushegir et al. [13] recently published a study showing the feasibility of FSpJ on aluminum alloy AA2024 and carbon fiber-reinforced poly(phenylene sulfide) (CF-PPS) laminate. They observed a correlation between the bonding area of the consolidated polmer and the lap shear strength. The authors proposed a simple model showing different bonding zones and their contribution in the joint strength. Esteves et al. [14] demonstrated that FSpJ can be used to join carbon fiber-reinforced PPS with aluminum alloy AA6181-T4. They demonstrated that the joint mechanical performance can be increased approximately 160% by performing metal surface pre-treatment to increase adhesion forces.

The previous publications have focused on case studies and technical feasibility of FSpJ process, with little or absent information on the influence of the FSpJ main process parameters on the microstructure and mechanical performance of the joints. The design of experiment approach designed by Taguchi [15] is a powerful statistical method that enables optimizing the performance of a product, process, design and system with a significant reduction in experiments, time and costs [16]. This method has already been successfully used in several studies on the optimization of welding processes. When combined with the use of analysis of variance (ANOVA), Taguchi models can be used to determine the relative importance of each joining process parameter on joint properties [16].

Campanelli et al. [17] investigated the effect of friction spot welding process parameters on the

shear strength of AZ31 magnesium alloy joints using Taguchi. They showed that plunge depth has the major effect on the weld strength, followed by rotational speed and dwell time. Pannerselvam et al [18] used the Taguchi method to optimize the shear strength of glass fiber-reinforced polypropylene laminate joined by resistance welding. The parameters analyzed were welding current, clamping pressure and welding duration. The welding current had the largest influence on the shear strength followed by time and pressure. Bilici [19] has achieved an improvement of 48% in the weld strength of friction stir spot welded polypropylene joints through the use of Taguchi method to optimize the joining parameters.

In this work, the Taguchi design of experiments method and ANOVA were used to investigate the individual influence of each FSpJ process parameter (rotational speed, plunge depth, joining time and joining force) on the microstructure and lap shear resistance of aluminum AA6181-T4 and carbon fiber-reinforced poly(phenylene sulfide) (CF-PPS) double-lap joints. Rotational speed, followed by joining time and plunge depth, presented the highest influence on lap shear strength of double-lap joints, while the joining force the lowest influence. Analysis of variance indicated that, the larger the joining time (larger heat inputs), plunge depth (bigger macro-mechanical interlocking) and joining force, the higher the joint strength was. An upper limit for the rotation speed was identified, where further increases resulted in smaller joint strengths (due to tool slippage decreasing heat generation) related to smaller bonding areas. Increasing of joining force led to better spreading (squeeze flow) of the molten polymer at the interface, resulting in a better crevice and pore filling at the metal surface; as a result adhesion forces and joint mechanical strength were improved.

2. Materials and methods

2.1. Aluminum AA6181-T4

Rolled aluminum AA6181-T4 sheets with thicknesses of 1.0 and 1.5 mm were used in this work. The aluminum AA6181 has silicon and magnesium as main alloying elements [20]. Although the alloys of 6xxx series are not as strong as most 2xxx and 7xxx series alloys, they possess good formability, weldability, machinability, and corrosion resistance, showing medium strength [21]. These alloys are usually used for car body inner and outer applications [22]. Table 1 lists the nominal chemical composition of the AA6181-T4 used in this work.

Table 1: Chemical composition of aluminum AA6181

Element	Si	Mg	Fe	Zn	Al
Wt%	0.85	0.78	0.25	0.11	bal

The heat treatment T4 consists in the solution of the precipitates in the alloy at high temperatures (515 – 570°C) followed by natural aging soon after rolling [23]. The main alloying elements, magnesium and silicon, combine to form the β-Mg_2Si precipitates [24], responsible for the alloy hardening. Table 2 lists selected physical and mechanical properties of AA6181-T4.

Table 2: Selected physical and mechanical properties of AA6181-T4 alloy [20,22]

Tensile Strength (direction TL) (MPa)	Yield Strength (direction TL) (MPa)	Elongation (%)	Density (g/cm^3)	Liquidus Temperature (°C)
267	161	25	2.7	645-655

2.2. Carbon fiber-reinforced poly(phenylene sulfide) composite laminate (CF-PPS)

A 2.17-mm-thick PPS laminate reinforced with 43 wt% of 5-harness (5H) satin weave carbon fibers (Tencate, the Netherlands) was used in this work [25]. The stacking sequence of carbon fiber layers followed the configuration $[(0.90)/(\pm45)]_3/(0.90)$. The relevant physical and mechanical properties of CF-PPS for this work are listed in Table 3.

Table 3: Selected physical and mechanical properties of PPS-CF at room temperature [25]

Tensile Strength (warp) (MPa)	In-plane shear strength (MPa)	Density (g/cm^3)	Glass transition temperature (°C)	Melting Temperature (°C)
758	119	1.35	120	280

2.3. Experimental procedure

Prior to joining, the aluminum specimens were slightly dry ground with P1200 SiC sandpaper to remove the weak and inhomogeneous natural oxide layer. Joining parts were cleaned with acetone to remove surface contaminations. The mechanical performance of the joints was evaluated by tensile shear test in accordance with ASTM D3528 [26] using double lap shear (DLS) joint specimen geometry (Figure 2). This configuration reduces the gross joint rotation responsible to create bending moment leading to peak shear stress at the edges of the overlap area. In this way DLS joints usually displays higher strengths than single-lap joints [27]. Lap shear testing was performed using a universal testing machine Zwick-Roell model 1478 with crosshead speed of 1.27 mm/min at room temperature. Five replicates were tested for each condition, and the ultimate lap shear force (ULSF) was calculated as the arithmetic mean of the five replicates.

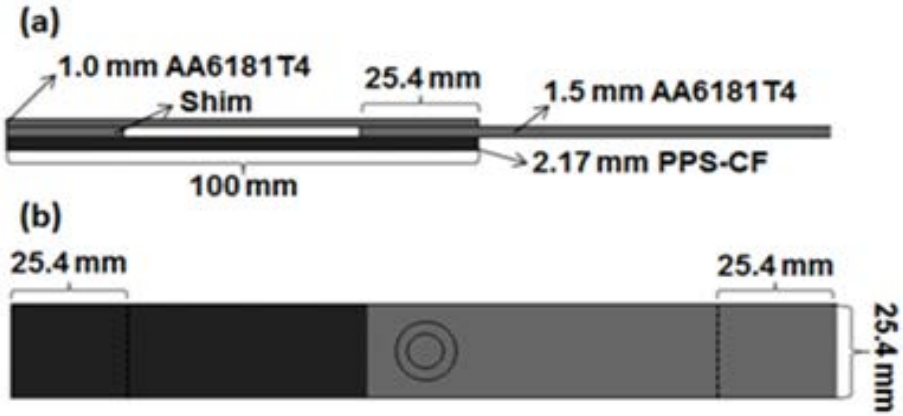

Figure 2: (a) Side view and (b) Top view of the double-lap joint configuration.

Cross sections were extracted from the center of the joint and embedded in low-temperature

cure epoxy resin for materiallographic preparation. Specimens were ground and polished following standard procedures. Light optical microscopy under reflective light (DM IR microscope, Leica, Germany) was conducted to examine the microstructure of the joints. To study the influence of joining process on joint mechanical strength, the bonding area was graphically measured at the surface of fractured double-lap shear specimens. For simplification purposes – Goushegir et al. [13] showed that bonding area has complex individual zones with different strengths - the bonding area was measured from the perimeter of the imprint left by the thin polymeric molten layer at the composite partner (Figure 3a). The metallic nub area was measured from the annular impression at the fractured surface at the metallic plate. An area of maximum deformation related to the sleeve plunging action (A1, Figure 3b) was subtracted from the central area bellow pin (A2, Figure 3b). The obtained are was used to evaluate the size modifications of the metallic nub.

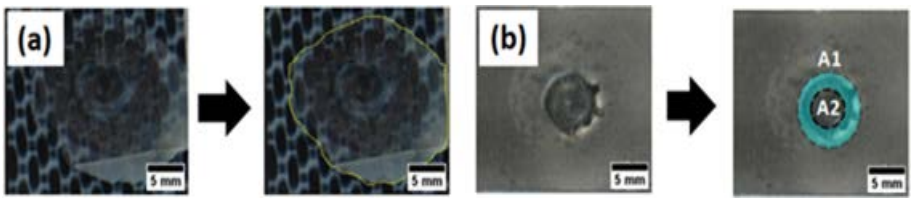

Figure 3: Example of (a) bonding area and (b) metallic nub area measurements.

2.4. Process optimization

The influence of the FSpJ process parameters on the mechanical performance of the joints was analyzed using Taguchi design of experiments (DoE) and ANOVA. The parameters and the levels evaluated are listed in Table 4. The studied response was the ULSF of the joints. The L9-orthogonal matrix consists of four columns and nine rows which resulted in nine experiments. This DoE – developed to decrease the numbers of experiments of a 3^4-full factorial model with 81 conditions [15] – has been used in welding to evaluate joint strength [17,19]. The range of welding parameters (levels), as the input for Taguchi experiments, was selected by preliminary microstructural analysis to evaluate joint formation (i.e. size of bonded area, presence of thermal volumetric flaws in the consolidated polymer, cracks in the aluminum partner), using the one-factor-at-a-time (OFAT) approach corresponding to the variation of a single parameter at a time. The statistical evaluation criterion chosen was “the-larger-the-better" for the S/N ratio (signal-to-noise) aiming at the determination of the maximal value of the response (ultimate lap shear force).

Table 4: FSpJ process parameters used in the Taguchi L9 matrix (3^4)

Symbol	Welding Parameter	Units	Level 1	Level 2	Level 3
RS	Rotational Speed	rpm	1200	1400	1600
PD	Plunge Depth	mm	0.75	1.00	1.15
JT	Joining Time	s	2	4	6
JP	Joining Force	kN	6.8	7.5	8.3

The S/N ratio for the larger-the-better analysis (S/N_{ltb}) was calculated using the Equation 1 [28]:

$$S/N_{ltb} = -10\log\left(\frac{1}{n}\sum_{i=1}^{n}\frac{1}{y_i^2}\right) \qquad (1)$$

where *n* is the number of tests and *y* is the value of ULSF of the *i-th* test.

3. Results and Discussion

3.1. Preliminary study on joining parameters: One-factor-at-time-a-time approach

OFAT approach was carried out to study the joinability of the aluminum alloy AA6181-T4 and CF-PPS laminate by FSpJ. This methodology was additionally used to refine the range of variation for each joining parameter as the input for the Taguchi experiments. Three levels were chosen for each parameter based on the presence of joint formation observed from the microstructural analysis. As an example of this procedure, the influence of plunge depth on the microstructure of FSp joints is discussed in this paper.

Four levels of plunge depth were analyzed: 0.75 mm (Figure 4a), 1.00 mm (Figure 4b), 1.15 mm (Figure 4 c) and 1.25 mm (Figure 4 d). The other joining parameters were fixed (RS: 1200 rpm, JT: 4 s and JF: 6.8 kN). Excessive plunge depth may cause defective joints with a geometrical feature called broken stir zone (BSZ). In these joints the central region of the aluminum plate under the pin is broken and removed due to excessive penetration of the sleeve, as can be seen in Figure 4d. The removed aluminum frequently remains attached to the pin during last step of the process (Figure 1b – 3). The schematic representation with the present explanation of the BSZ defect formation is illustrated in Figure 5. From our current understanding, fracture of the aluminum plate during BSZ formation locally occurs due to the temperature-related increase in formability; the load imposed by the plunging sleeve exceeds the local metal strength inducing cracking. Further studies with finite element modeling to determine the complex stress distribution behavior culminating in the formation of BSZ is out of the scope of this paper and will be published in a separate manuscript.

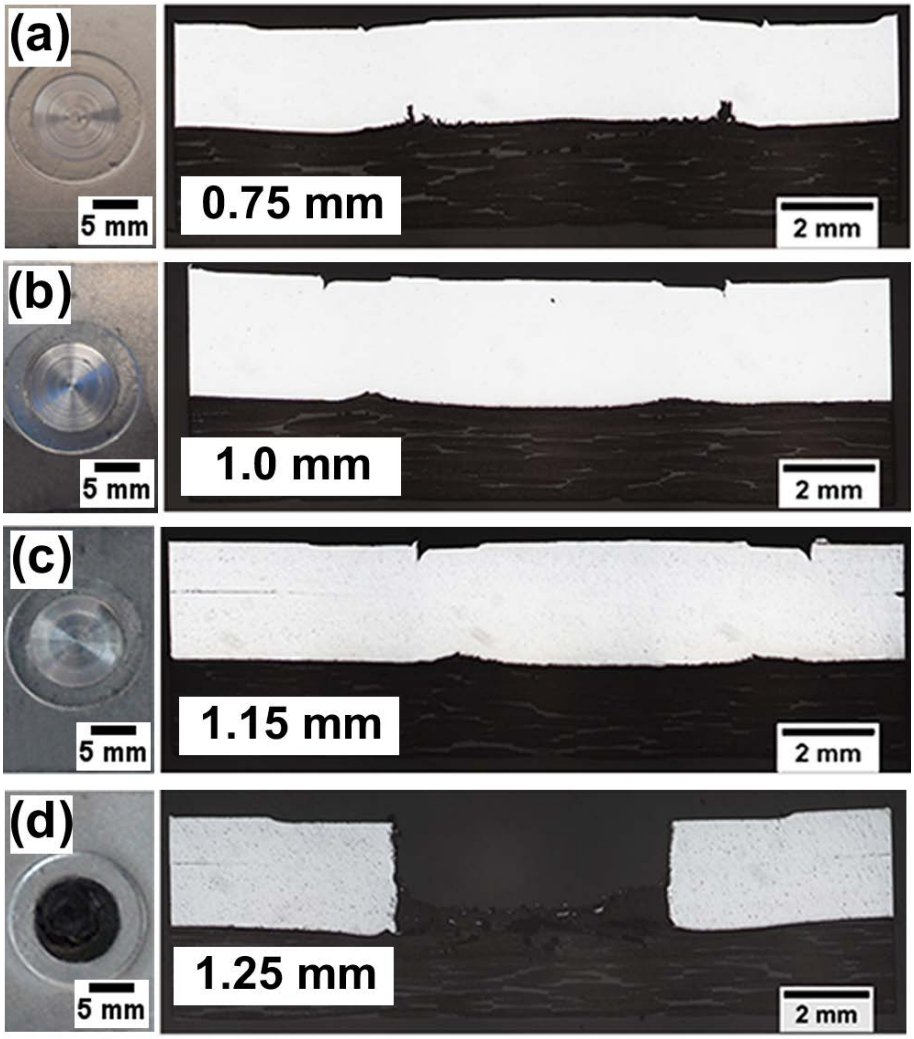

Figure 4: Top view (left-hand side photos) and mid cross-section micrographs (right-hand side photos) of samples joined at plunge depth (PD): (a) 0.75 mm, (b) 1 mm, (c) 1.15 mm and (d) 1.25 mm and constant RS of 1200 rpm, JT of 4 s and JF of 6.8 kN.

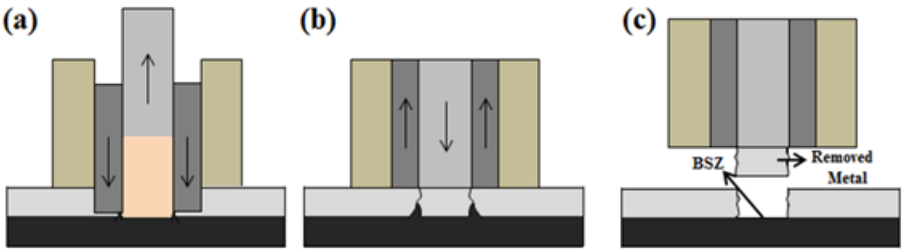

Figure 5: Broken stir zone occurrence process: (a) the sleeve plunge depth is achieved and the crack nucleates; (b) crack propagates through plate thickness under the pin during the sleeve retraction an refilling of the plasticized material kept in the formed reservoir between sleeve and pin; (c) the central region of the joint fractures usually remaining attached to the pin.

From the microscopical analysis in Figure 4, one can conclude that the plunge depth of 1.25 mm led to the generation of defective joints. Therefore the maximum PD level to be used in the Taguchi L9 study for plunge depth was set to 1.15 mm while the minimum level to 0.75 mm and the mean level to 1.0 mm. The range (see Table 4) for the rotational speed, joining time and joining force was selected following a similar procedure as for plunge depth. These results will be published in a separate document.

3.2. Influence of FSpJ process parameters on joint mechanical performance: Taguchi design of experiment

Table 5 lists the Taguchi orthogonal array for the FSpJ parameter combinations along with the experimental mean values and the standard deviations of the ULSF and the S/N ratios for the AA6181-T4 / CF-PPS double lap shear joints. The S/N ratio indicates how much the quality characteristic ULSF deviates from the desired value. The higher is the S/N ratio the better is the investigated response [15].

Table 5: Experimental mean values and standard deviation of ULSF and S/N ratios for AA6181-T4 / CF-PPS joints as a function of the FSpJ parameters

Condition	RS (rpm)	PD (mm)	JT (s)	JF (kN)	ULSF(N)	S/N ratio (dB)
1	1200	0.75	2	6.8	2107 ± 470	65.85
2	1200	1	4	7.5	2480 ± 286	67.75
3	1200	1.15	6	8.3	3523 ± 527	70.69
4	1400	0.75	4	8.3	3241 ± 662	69.68
5	1400	1	6	6.8	3460 ± 381	70.65
6	1400	1.15	2	7.5	3254 ± 485	69.97
7	1600	0.75	6	7.5	3153 ± 282	69.88
8	1600	1	2	8.3	3112 ± 523	69.47
9	1600	1.15	4	6.8	3248 ± 722	69.63

The joints exhibited shear forces ranging from 2107 N (condition 1) to 3523 N (condition 3). The joints show displacement-at-peak load values from 0.7 mm (condition 1) to 0.9 mm (condition 3), indicating a brittle fracture. Conditions 1 and 2 show the lowest values for ULSF perhaps because of the lower heat input, as it will be discussed within this section. All remaining FSpJ conditions (3 – 9) led to similar ULSF values taking into account the overall mean ULSF value (3064 ± 466 N) and the standard deviations of each joint condition tested.

Condition 3 shows the highest S/N ratio as a result of the selected combination of process parameters leading to high heat input and large plunge depth. Based on the similarities of FSpJ and other friction-based welding processes concerning the heat generation, the thermal model of Equation 2 for the friction stir spot welding (FSSW) [29] was used to better understand the effect of the FSpJ process parameters on joint mechanical behavior.

$$Q = \sum_{n=1}^{n=N} M(n)\omega(n)\Delta t \qquad (2)$$

, where M is the torque (N.m), ω is the rotational speed (rad/s) of the tool, Δt is the joining time, and n refers to the experiment number.

One can observe from Equation 2 that rotational speed and joining time are important variables for the heat generation. The larger these parameters, the larger the heat input. Higher heat input induces the formation of large bonded areas, as visually confirmed by a large amount of PPS molten layer at the interface. This can be seen in the fracture surface of condition 3 in Figure 6a (indicated by white arrows) in comparison to condition 1 (Figure 6b).

Furthermore, pronounced nub formation was observed in condition 3 due to the combination of large heat input (RS : 1200 rpm; JT: 6s) and plunge depth (1.15 mm) (black arrows, Figure 6c), while for condition 1 nub formation was almost inexistent due to combined lower heat input (RS: 1200 rpm; JT: 2s) and smaller PD of 0.75 mm (black arrows, Figure 6d).

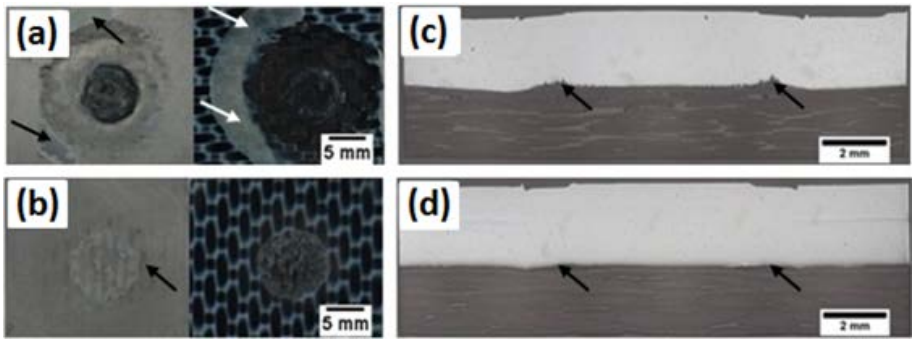

Figure 6: Fracture surface of the joints after lap shear testing: (a) condition 3; (b) condition 1. Macrostructure of the joint cross-section: (c) condition 3; (d) condition 1.

The fracture of conditions 1 and 3 occurred predominantly by adhesive (at the interface between aluminum and consolidated polymeric layer) and cohesive (within the thickness of the consolidated polymeric layer in the top composite plies [13]) failures, respectively. In the cohesive failure, the PPS consolidated layer remains partially attached to the aluminum and the composite plates. Condition 1 shows the lowest S/N ratio in the experimental set-up, due to its low thermal contribution as a result of the selected combination of process parameters (combination of minimum values of RS and JT); it induced the formation of a smaller PPS molten layer and adhesion forces at the interface. Therefore a smaller bonded area was formed reducing mechanical strength. Moreover condition 1 was performed with the lowest level of plunge depth (0.75 mm) reducing the formation/size of the nub and the additional macro-mechanical interlocking, as indicated by the black arrows in Figures 6b and 6d.

Orthogonal array design of Taguchi experiments allows analyzing the individual effect of each FSpJ process parameter on joint strength. The mean values of the S/N ratio for each process parameter at levels 1 (minimum), 2 (mean) and 3 (maximum) were calculated for ULSF from the S/N ratio values listed in Table 6. The maximum difference between the mean S/N ratio values in the three tested levels (delta max) was calculated from the data of Table 5 for each parameter. This difference indicates how sensitive is the response of ULSF to the variation of a given joining parameter, allowing ranking the individual importance for each joining parameter.

Table 6: Main effects of the S/N ratio

Level	**RS**	**PD**	**JT**	**JP**
1	68.1	68.47	68.43	68.71
2	70.1	69.29	69.02	69.2
3	69.66	70.09	70.41	69.94
Delta max	2	1.62	1.98	1.24
Rank	1	3	2	4

Figure 7 is a more complete graphical representation of Table 6 illustrating the main effects plots for S/N ratio. The dashed line represents the total mean value for S/N ratio, which was calculated as 69.3 db (dash line in Figures 7a-d).

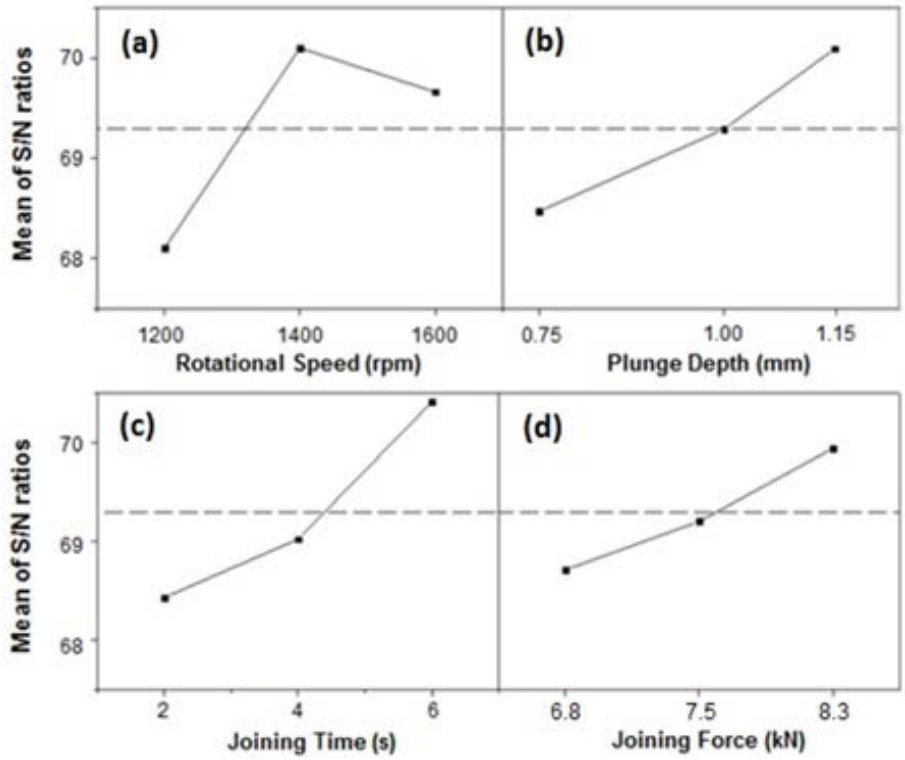

Figure 7: Main effect plots for S/N ratio for each FSpJ process parameter: (a) rotational speed; (b) plunge depth; (c) joining time; (d) joininig force.

According to Table 6 and Figure 7, the rotational speed has the greatest effect on the lap shear strength of the joints, followed by joining time, plunge depth and joining force (the larger the curve slopes, the bigger the influence of a joining parameter). The effect of the most important process parameters - rotational speed and joining time - on the mechanical strength of the joints shows that the heat input plays a major influence on the bonding mechanisms because it is responsible for the level of melting/softening of the PPS matrix at the interface. In addition to this effect, the plunge depth promotes the formation of macro-mechanical interlocking of the sheets through plastic deformation of the metal and formation of the nub. Therefore, the control of the heat input and plunge depth is crucial in obtaining strong joints.

ANOVA was carried out to define the relative importance of each FSpJ process parameter on the ULSF of the joints. The contribution percentage P% was calculated by the ratio of the sum of squares (SS) of the selected factor and total sum of squares. Table 7 lists the ANOVA results of S/N ratio. The error was not considered by the statistical model in this case since the degree of freedom of the error is zero. The mean square (MS) is calculated by the sum of squares divided by the number of degrees of freedom associated with the respective process parameter.

Table 7: ANOVA for S/N ratio of ULSF

Source	DF	SS	MS	P%
RS	2	6.65	3.33	34.77
PD	2	3.96	1.98	20.70
JT	2	6.19	3.10	32.37
JF	2	2.32	1.16	12.15
Error	0	-	-	-
Total	8	19.13	-	100

SS - Sum of squares, DF - Degree of freedom, MS - Mean square, P% - Percentage of contribution %

The results showed in this table is in agreement with the results obtained in Table 6 in which the tool rotational speed (34.77%) is the most important process parameter changing the ULSF, followed by joining time (32.37%), plunge depth (20.70%) and joining force (12.15%).

The individual influence of the FSpJ process parameters on the joint strength and microstructure were individually analyzed and discussed into more details in the following sections.

A) Rotational speed (RS) and Joining Time (JT)

In the graph shown in Figure 7a the shear force - represented by S/N ratio - increases with the rotational speed from 1200 to 1400 rpm. This can be attributed to the increase in the heat input, which results in larger bonded areas (changes in the perimeter of the bonding area in Figure 8a and b) and therefore higher mechanical performance. Such behavior was already reported by Goushegir et al. [13] in friction spot joining of AA2024 / CF-PPS. The authors showed that bonded area increases continuously by increasing the rotational speed of the tool due to higher heat input, therefore leading to higher joint mechanical performance. In contrast to their findings, the lap shear strength of the joints in this study decreased at rotational speeds higher than 1400 rpm. This behavior may be explained by the well-known tool slip phenomenon, usually observed during the welding of aluminum by friction stir spot welding (FSSW) [30, 31]. The increase in temperature, when further elevating rotational speeds, leads either to the reduction of the plasticized aluminum viscosity and/or local melting [31] (the latter was not detected in this study). When RS is changed from 1400 to 1800 rpm slippage between the tool and the surrounding aluminum may take place. This decreases the torque and reduces the frictional heat generation (Equation 2) leading to smaller bonding areas and decreasing the joint strength (Figures 8 and 9).

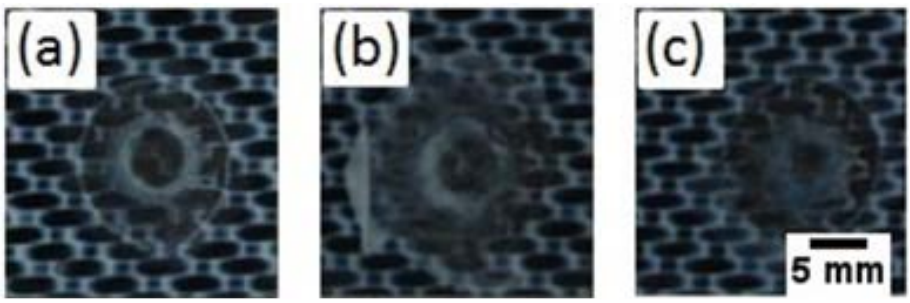

Figure 8: Fracture surfaces of samples joined at rotational speeds (RS): (a) 1200 rpm, (b) 1400 rpm and (c) 1600 rpm.

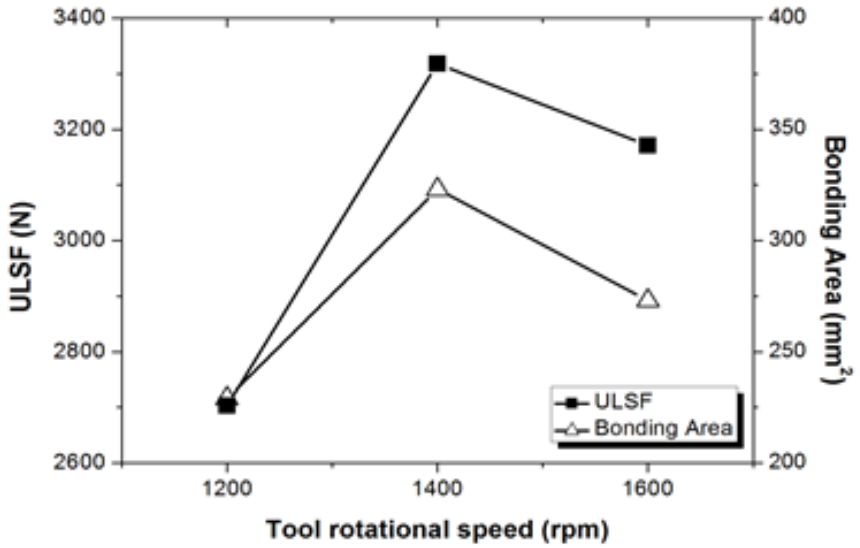

Figure 9: Influence of the tool rotational speed (RS) on the ULSF and bonding area.

According to Table 6 and ANOVA results, joining time is the second parameter with highest influence on the mechanical performance of the joints. For the same reasons discussed for the rotation speed, increase of the joining time within the analyzed interval (2 – 6 s) increases the bonding area and the lap shear strength (Figures 10 and 11).

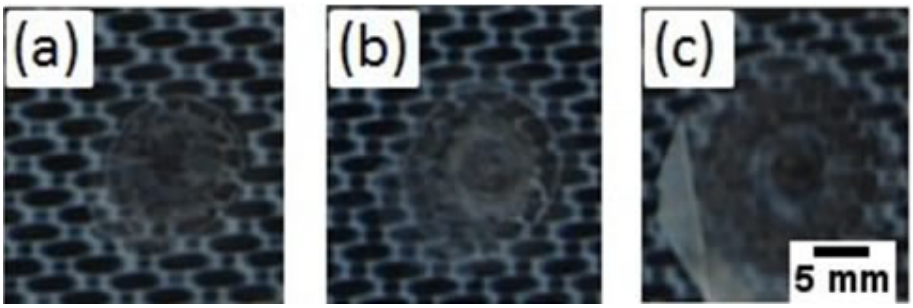

Figure 10: Fracture surfaces of samples joined with joining time (JT): (a) 2 s, (b) 4 s and (c) 6 s.

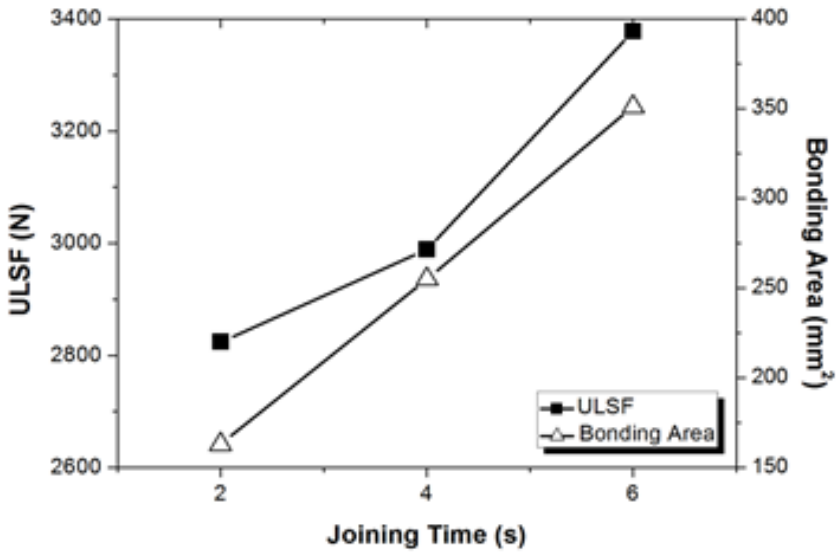

Figure 11: Influence of the joining time (JT) on the ULSF and bonding area.

C) Plunge depth (PD)

As previously discussed in Figure 6, lap shear strength of friction spot joints is a combination of bonding area size and macro-mechanical interlocking related to the metallic nub. The increase in the plunge depth within the selected range augments the ULSF (Figure 7 b and Figure 12) owing to the larger indentation of the aluminum into the composite surface (metallic nub) and macro-mechanical interlocking (Figure 13).

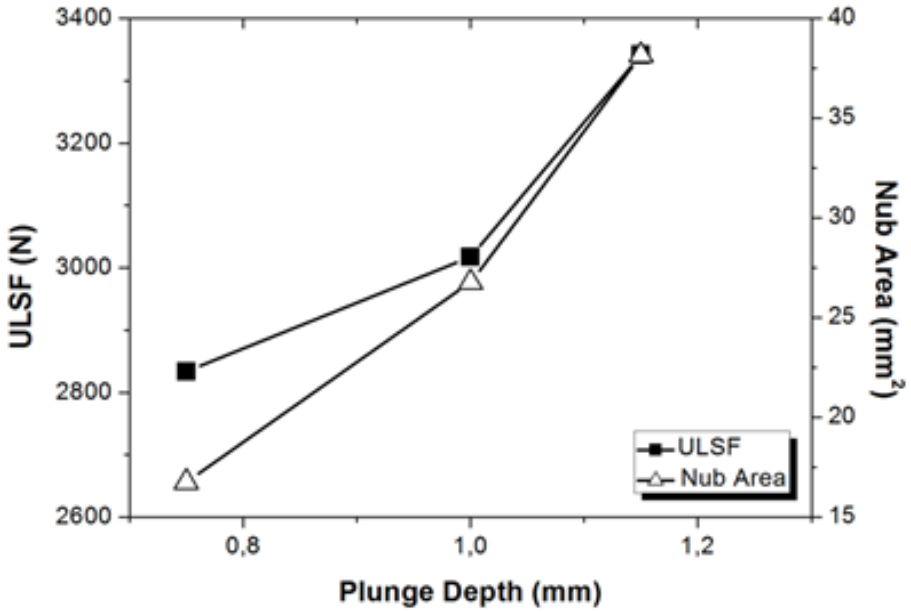

Figure 12: Influence of the plunge depth (PD) on the ULSF and nub area.

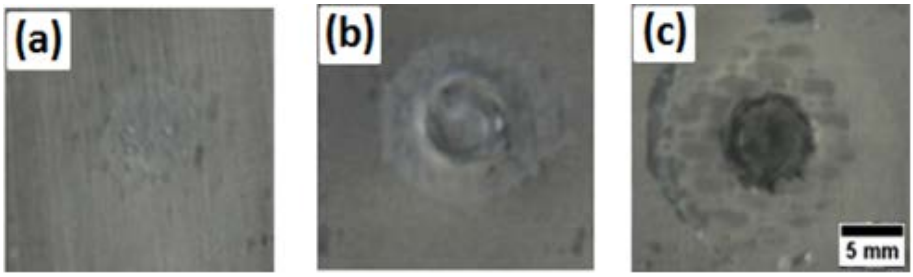

Figure 13: Fracture surfaces of samples joined with plunge depth (PD): (a) 0.75 mm, (b) 1.00 mm and (c) 1.15 mm.

The mechanisms dictating the formation of the metallic nub are still not well understood, however current theory states that size and shape will be directly influenced not only by plunge depth, but also by the local metal formability. Therefore different heat input levels may change the final geometry of the metallic nub, at same plunge depths. For example, condition 1 (Fig. 14a) and condition 7 (Fig. 14b) of the Taguchi orthogonal array L9 (Table 2) have the same level of plunge depth (0.75 mm). Nevertheless, condition 7 was joined with higher heat input (RS: 1600 rpm and JT: 6 s) compared to condition 1 (RS: 1200 rpm and JT: 2 s) increasing aluminum formability (more pronounced metallic nub, see black arrows in Figure 14b) and bonding area (white arrows, Figure 14b), resulting in higher mechanical strength as shown in Figure 14c

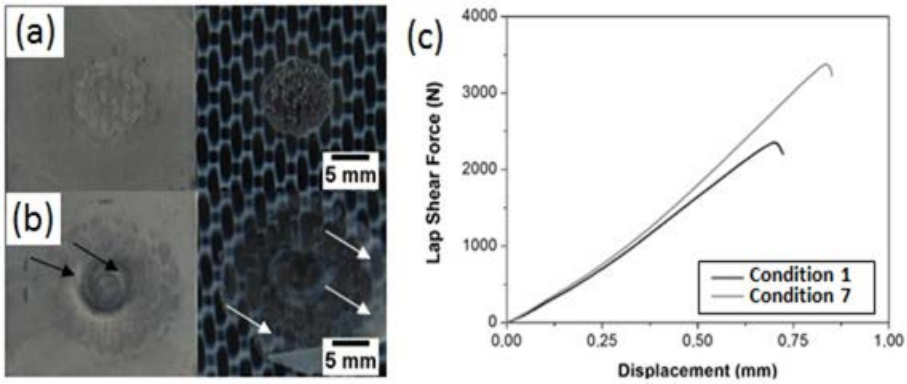

Figure 14: (a) Fracture surface of condition 1; (b) Fracture surface of condition 7 and (c) Load-displacement curves in lap shear testing for conditions 1 and 7.

D) Joining Force (JF)

For the selected materials and studied range of process parameters, lap shear strength showed the smallest sensitivity to the variation of the joining force, as illustrated in Figure 7 and Table 7. Bonding micro-mechanisms at the interface metal-composite were recently reported in [13]. Hydrostatic forces created as a result of the applied JF mainly control flow of molten polymer and pore filling at the aluminum surface. Higher JF are expected to increase spreading of the molten polymer layer onto the crevices and pores of the metal surface improving wettability (pore filling) at the interface. Therefore micro-mechanical interlocking efficiency will increase supporting better mechanical performance (see Figure 7d). On the other hand, excessive JF can decrease molten layer thickness by pushing off molten polymer outside the bonding area (squeezing flow). Very thin layers will decrease adhesive forces at the interface, leading to lower strengths. In this work the selected range of JF obtained through the OFAT analysis was

optimized to allow joint formation. In this way, significant differences in the mechanical performance of the samples were not observed. Further studies within larger ranges of joining forces are required to further understand this behavior.

4. Conclusions

The individual effect of the friction spot joining (FSpJ) process parameters on the microstructure and mechanical strength of aluminum AA6181-T4 / carbon fiber-reinforced poly(phenylene sulfide) laminate (CF-PPS) hybrid joints was investigated using statistical analysis. Produced joints showed good mechanical performance with ultimate lap shear forces varying from 2107 N (condition 1) to 3523 kN (condition 3). Joints failed by brittle fracture (displacement-at-peak load values from 0.7 mm for condition 1 to 0.9 mm for condition 3), with a combination of adhesive and cohesive micro-failure at the interface.

The use of a Taguchi L9 (3^4) design of experiments and analysis of variance allowed the determination of the individual influence of the main joining parameters on joint lap shear resistance. Taguchi analysis indicated that the tool rotational speed is the parameter with the largest influence on the lap shear strength of the joints (34.77%), followed by the joining time (32.37%), plunge depth (20.70%) and joining force (12.15%). It was demonstrated that, the combination of rotational speed and joining time increases heat generation, changing joint microstructure and the lap shear strength. The level of the heat input is responsible for the amount of the PPS molten layer at the joint interface increasing bonding area. Moreover plunge depth plays an important role in the macro-mechanical interlocking mechanisms at the metal-composite interface controlling the formation of the metallic nub. The higher the plunge depth the more pronounced will be the metallic nub (Figure 6). Therefore larger heat inputs as a result of elevated joining times and optimized rotational speeds (there is a upper limit for the former, where increases in the latter will induce tool slippage, decreasing heat generation) as well as plunge depth, will lead to stronger joints. However, the plunge depth has a limitation since too large plunge depths can cause the rupture of the aluminum plates within the spot joint area. Defective joints will be formed with the central spot area being removed creating the so-called broken stir zone (Figure 4d), reducing joint mechanical strength.

The current study showed that the typical tool slippage phenomenon associated with higher rotational speeds changes heat generation regime, as found in friction-based metal welding processes. Higher rotational speeds will decrease the viscosity of plasticized metal, decreasing heat generation. As a result smaller bonding areas will be created, reducing mechanical performance. Joining time has a similar behavior as the rotational speed. The longer the joining time the stronger will be the joints due to larger bonded areas. Plunge depth of the tool is another important parameter for the joint lap shear force. Increases in plunge depth resulted in higher macro-mechanical interlocking, due to the larger indentation of the deformed aluminum (metallic nub) in the composite, leading to better mechanical performance.

A direct correlation of joining force with pore filling was identified. Joining force supports spreading of the molten polymer on the metallic surface. Thus increasingly joining forces will lead to better wetting of the interface increasing adhesive forces. Nevertheless excessive joining forces can cause squeezing flow of the molten layer reducing the joint strength, since a large adhesive area is lost. This preliminary work contributed to the further understanding of the relationship between joining process parameters on microstructure and mechanical performance

of friction spot joints. However more elaborate design of experiments and process computational modeling should be applied to better understanding the secondary and other combined interaction of joining parameters on joint mechanical performance.

Acknowledgements

The authors would like to acknowledge the financial support of Helmholtz Association (Young Investigator Group “Advanced Polymer-Metal Hybrid Structures”), Germany and CNPq - National Council for Scientific and Technological Development, Brazil (MSc scholarship of J.V. Esteves).

5. References

[1] Blawert C, Hort N., Kainer K.V. Automotive applications of magnesium and its alloys. Trans Indian Inst Met 2004;57:397-408.

[2] Davies G. Future trends in automotive body materials. Mater Automob Bodies 2003;8:252-269.

[3] Matsuyama K. Trend of automobile vehicles and joining technologies. Inter Weld Ins Doc IIW - Doc III 2006;06:1386.

[4] Yousefpour A., Hojjati M., Immarigeon J.P. Fusion bonding/welding of thermoplastics composites. Journa of thermoplastic Composite Materials. 2004;17:303.

[5] Faupel F., Willecke R., Thran A. Diffusion of metals in polymers, Mat. Sci. Eng. 1998;22:1-55

[6] Amancio-Filho S.T., dos Santos J.F. Joining of polymers and polymer-metal hybrid structures: Recent developments and trends. Polym. Eng. Sci. 2009;49 (8):p 1461–1476.

[7] Amancio Filho S.T., dos Santos J.F. Method for joining metal and plastic workpieces. European Patent EP 2329905 B1, 2012.

[8] Rosendo T.S., Parra B., Tier M.A.D., da Silva A.A.M., dos Santos, J.F. Strohaecker, T.R., Alcantara, N.G. Mechanical and microstructural investigation of friction spot welded AA6181-T4 aluminum alloy. Materials in Engineering 2011;32:1094-1100.

[9] Amancio-Filho S.T., Camillo A.P.C, Bergmann L., dos Santos J.F., Kuri S.E. Alcantara N.G. Preliminary Investigation of the Microstructure and Mechanical Behaviour of 2024 Aluminium Alloy Friction Spot Welds, Materials Transactions, 52 (5), 985-991, 2011.

[10] Oliveira P.H.F., Amancio-Filho S.T., dos Santos J., Hage Jr. E. Preliminary study on the feasibility of friction spot welding in PMMA. Materials Letters 2010;64:2098-2101.

[11] Gonçalves J, dos Santos J.F., Canto L.B., Amancio-Filho S.T., Improvement of the Friction Spot Welding (FSpW) to join Polyamide 6 and Polyamide 66/Carbon Fiber Laminate. Soldagem & Inspeçao accepted for publication on 17th February 2014.

[12] Amancio-Filho S.T., Bueno C., dos Santos J.F., Huber N., Hage JR. E., Hoppe A. On the Feasibility of Friction Spot Joining in Magnesium/Fiber-reinforced Polymer Composite Hybrid Structures. Mat. Sci. Eng.A 2011 A;49(8):1461–1476.

[13] Goushegir S.M., dos Santos J.F, Amancio-Filho S.T. Friction spot joining of aluminum AA2024/carbon fiber-reinforced poly(phenylene sulfide) composite single lap joints: microstructure and mechanical performance. Materials and Design 2014;54:196-206.

[14] Esteves J.V., Amancio-Filho S.T., dos Santos J.F., Canto L.B., Hage Jr. E. Friction spot joining of aluminum 6181-T4 and carbon fiber-reinforced poly(phenylene sulfide) . In Proc.: ANTEC 2012, Society of Plastics Engineers, April 2012, Orlando, FL, EUA, paper No. 418.

[15] Taguchi G., Chowdhury S., Wu Y. Taguchi's Quality Engineering Handbook, NJ: John Wiley & Sons, Inc., 2005.

[16] Montgomery D.C. Design and analysis of experiments, 4th ed. NY: John Wiley & Sons, Inc, 2006.

[17] Campanelli L.C., Suhuddin U.F.H., dos Santos J.F., Alcantara N.G. Parameters optimization for friction spot welding of AZ31 magnesium alloy by Taguchi method. Sold. Insp. 2012;17(1).

[18] Panneerselvam K., Aravindan S., Noorul H. Study on resistance welding of glass fiber reinforced thermoplastic composites. Materials and Design. 2012, 41: 453-459.

[19] Bilici M.K. Application of Taguchi approach to optimize friction stir spot welding parameters of polypropylene.Materials and Design. 2012, 35: 113-119.

[20] ASM International. ASM Handbook: Properties and Selection: Nonferrous alloys and special-purpose materials. v.2, 1992.

[21] Callister JR. W. D. Materials Science and Engineering: an introduction. 7th ed., John

Wiley & Sons, 2007.
[22] European Aluminum Association. Applications - Car Body - Body structures. The Aluminum Automotive manual, 2013.ASM International.
[23] ASM Handbook: Heat Treating. v. 4, 1991.
[24] Milkereit B., Wanderka N., Schick C., Kessler O. Continuous cooling precipitation diagrams of Al-Mg-Si alloys. Materials Science and Engineering A. 2012, 550: 87-96.
[25] Tencate composites. CETEX-PPS Guide Lines, 2011.
[26] ASTM D3528-96, Standard test method for strength properties of double-lap shear adhesive joints by tension loading. ASTM International, 2008.
[27] Packham D.E. Handbook of adhesion. 2. Ed. John Wiley & Sons, Ltd.,2005.
[28] Minitab. Taguchi Designs. Minitab user's guide. vs.2, 1-39, 2010.
[29] Su P. et al. Energy generation and stir zone dimensions in friction stir spot welds. SAE Technical Paper, 2006-01-0971, 2006.
[30] Gerlich A., Su P., North T. Peak temperatures and microstructures in aluminum and magnesium alloy friction stir spot welds. Science and technology of welding and joining, vol 10, 2005.
[31] Gerlich, A. Yamamoto, M. North, T. Local melting and tool slippage during friction stir spot welding of Al-alloys. J. Mater Sci. 2008, 43: 2-11.